Effect of surface texture and geometry on spoof surface plasmon dispersion

Shun-Hui Yang
Prabhakar R. Bandaru
University of California, San Diego
Materials Science Program
Department of Mechanical and Aerospace Engineering
La Jolla, California 92093-0411

Abstract. The possibility of light manipulation at the nanoscale relies on the efficient coupling of the electromagnetic waves to surface excitations such as surface plasmon polaritons (SPPs). We expand on the work by Pendry, who put forward the idea of spoof surface plasmons in conducting films as a way to engineer SPP dispersion curves. We find that the surface texture and geometry can play an important role in determining the dispersion. We then compare the specific cases of circular versus rectangular textured surfaces and observe that the plasmon modes are less tightly bound in the former case. This dependence on geometry can also be used as a means for defect engineering or fine-tuning the regular plasmon dispersion. *© 2008 Society of Photo-Optical Instrumentation Engineers.*
[DOI: 10.1117/1.2844723]

Subject terms: surface plasmon polaritons (SPPs); dispersion curves; defect engineering.

Paper 070508R received Jun. 20, 2007; revised manuscript received Sep. 18, 2007; accepted for publication Oct. 1, 2007; published online Feb. 21, 2008.

The field of plasmonics[1] is concerned with the manipulation of electromagnetic waves in the subwavelength regime. In addition to new insights into nanoscale optics, such as higher than expected transmission in subwavelength hole arrays,[2] this field has formed the basis for sensors,[3] diagnostics at the single molecule level through surface enhanced Raman scattering (SERS),[4,5] nanolithography,[6] directed light sources,[7] and higher efficiency[8] light emitting diodes (LEDs). In devices exploiting plasmonic phenomena, external light (typically, of TM mode polarization[9]) is coupled to a substrate, and a bound surface electromagnetic mode, the surface plasmon polariton (SPP), is excited. While the exact influence of the SPPs in optical phenomena such as enhanced optical transmission is under dispute[10,11] due to possible contributions[11,12] from Fabry-Perot, waveguide-mode, cavity-mode, and structural[13] resonances, with some reports even attributing a negative role,[14] an investigation of their phenomenology would still yield insight into the localization and guiding of electromagnetic energy.[15] The SPP propagation could be directed and manipulated through waveguides and couplers.[16] However, due to the bound nature of the SPP, there is a momentum mismatch (manifested through a **k**-vector difference) with the free-space light photon, which, as we show in this paper, depends sensitively on the nature of the surface. While this mismatch in principle can be overcome by using external grating couplers,[17,18] our work is pertinent in that it suggests ways to engineer the SPP dispersion curves. In light of the recent formulation[19] and experimental verification[20] of designer surface plasmons on conducting films, constructed through surface texturing, these possibilities could lead to a whole new array of optical devices.

0091-3286/2008/$25.00 © 2008 SPIE

In this paper, we look at the effect of surface geometry and arrangement on spoof SPP dispersion in more detail and note that the shape of the fundamental unit can also play a major role. For example, we find that SPPs are less tightly bound to a surface patterned with circular holes compared to a surface comprising square/rectangular holes due to a smaller momentum mismatch. The dispersion relations for these textured surfaces are formulated in a canonical plasmonic form,[19,21] enabling SPP engineering at any frequency and contributing to judicious design of metamaterials.

By solving the Maxwell equations on the surface of a semi-infinite conducting (M) film, bounded by a dielectric (D) medium, the SPP dispersion relation of an untextured conducting film is derived[17] as:

$$k_f = k_0\left(\frac{\varepsilon_D\varepsilon_M}{\varepsilon_D+\varepsilon_M}\right)^{1/2}. \quad (1)$$

Here, k_0 and k_f are the wave vectors of the electromagnetic field in vacuum and SPP mode, respectively. The dielectric constant for the dielectric film is represented through ε_D, and the frequency (ω)–dependent dielectric function for conducting film is $\varepsilon_M = 1-(\omega_p^2/\omega^2)$ where ω_p is the plasma frequency of the conducting film. It is hence observed that k_f is larger than k_0 when ω is less than ω_p; consequently, the electromagnetic field of SPP mode decays exponentially with distance from the surface. This field is said to be evanescent, and SPP mode is thus bound to the surface. We now look at the momentum mismatch between k_0 and k_f as manifested through the appropriate choice of texture and material. The rationale, following Pendry,[19] is to examine the plasmon dispersion as a function of subwavelength surface structure. This difference is clearly seen in the ω-k relation (Fig. 1) of textured surfaces in comparison to an unpatterned conducting film.

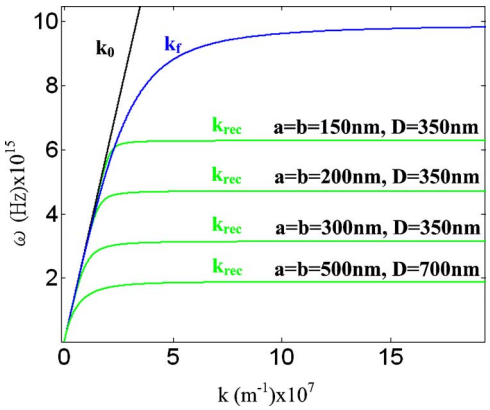

Fig. 1 Surface texture affects the details of (ω-k) dispersion of the bound surface plasmons. The plasmon frequency can be tuned by changing the geometry and material inside the holes. k_f represents the SPP wave vector of untextured conducting film, k_0 the free-space light line, and k_{rec} the wave vector of rectangular textured conducting film. (The calculations are for a conducting silver film).

For the case of rectangular holes of dimension $a \times b$ patterned in a conductor (Fig. 2), the electric field in the holes due to a plane wave (of wavelength λ and frequency ω) incident in the z direction has the form[19]:

$$E = E_0[0,1,0]\sin\left(\frac{\pi x}{a}\right)\exp[i(k_z z - \omega t)],$$

$$\text{where } 0 < x < a,\ 0 < y < b, \text{ and } a,b \ll \lambda. \tag{2}$$

This is the fundamental mode, and the electrical field is in the y direction. (In this paper, we consider *only* the lowest-order mode (TE_{10}), where the electric field (E) is parallel to the y axis. In this situation, along the y axis, the magnitude of E varies sinusoidally (with x) and is zero at both ends (x=0 and x=a), i.e., along two sides of the hole. A higher-order mode (say, TE_{11}) would incorporate sinusoidal variation along both x and y and would correspond to an E field of zero on *all* sides of the hole.

One can describe the response of the composite structure as an effective medium with dielectric constants (ε_y) and magnetic permeability coefficients (μ_x). We equate the incident field (E) and energies ($E \times H$) in the bare hole to the field and energy in the effective medium comprising the holes as:

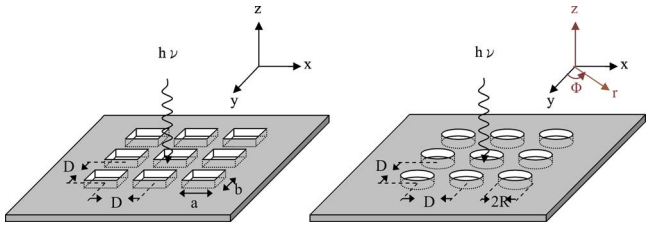

Fig. 2 The geometry of surfaces with rectangular (dimensions =a,b) and circular (diameter=2R) holes. Electromagnetic radiation is incident in the negative z direction onto the surface.

$$E_0 \frac{b}{D^2}\int_0^a \sin\left(\frac{\pi x}{a}\right)dx = E_0 \frac{2ab}{\pi D^2} = E_0', \tag{3}$$

$$\begin{aligned}(E \times H)_z &= \frac{-k_z E_0^2}{\omega \mu_h \mu_0}\frac{b}{D^2}\int_0^a \sin^2\left(\frac{\pi x}{a}\right)dx \\ &= (E' \times H')_z \\ &= \frac{-k_z E_0'^2}{\omega \mu_h \mu_x}.\end{aligned} \tag{4}$$

Here, E' is the electric field in the effective medium. From Eqs. (3) and (4), we derive the magnetic permeability coefficient to be

$$\mu_x = \frac{8ab\mu_h}{\pi^2 D^2}. \tag{5}$$

The k vector, in the z direction, is written as:

$$k_z = k_0(\varepsilon_y \mu_x)^{1/2} = \left(\varepsilon_h \mu_h k_0^2 - \frac{\pi^2}{a^2}\right)^{1/2}. \tag{6}$$

We then derive a dielectric dispersion relation for a conducting film with two-dimensional (2-D) periodic rectangular holes as:

$$\varepsilon_y = \frac{\pi^2 d^2 \varepsilon_h}{8ab}\left(1 - \frac{\pi^2 c^2}{a^2 \omega^2 \varepsilon_h \mu_h}\right). \tag{7}$$

This expression is analogous to a plasmon-like dispersion of the form $[1-(\omega_p^2/\omega^2)]$, with a plasma frequency (ω_{pr}).

$$\omega_{pr} = \frac{\pi c}{a(\varepsilon_h \mu_h)^{1/2}}. \tag{8}$$

ε_h and μ_h are the permeability and permittivity of the holes in the medium. It is seen that surface texturing provides a waveguide like[22] dispersion, and concomitantly, below a cutoff frequency/wavelength, bound states exist. These bound states were referred to by Pendry as spoof surface plasmons. From energy conservation across the interface i.e., $k_0^2 = k_{rec}^2 + k_{z'}^2$, where k_{rec} is the wave vector of the surface plasmon in the plane of the rectangular-textured surface and $k_{z'}$ is the evanescent wave vector into the medium) and Fresnel's reflection equation[17] [i.e., $r=(k_z' - \varepsilon_x k_z)/(k_z' + \varepsilon_x k_z) = \infty$], we derive the dispersion relation:

$$k_{rec}^2 c^2 = \omega^2 + \frac{\mu_h}{\varepsilon_h}\frac{64a^2b^2\omega^4}{\pi^4 D^4}\left(\frac{1}{\omega_{pr}^2 - \omega^2}\right). \tag{9}$$

If the electrical field is oriented in the x direction, the dispersion relation is:

$$\varepsilon_x = \frac{\pi^2 d^2 \varepsilon_h}{8ab}\left(1 - \frac{\pi^2 c^2}{b^2 \omega^2 \varepsilon_h \mu_h}\right), \tag{10}$$

$$\omega_{pr}' = \frac{\pi c}{b(\varepsilon_h \mu_h)^{1/2}}. \tag{11}$$

These equations are plotted in Fig. 1. The implication is that by varying the hole dimensions, we can tune the plasma frequency, i.e., decreasing the size, or the refractive index $[n=(\varepsilon_h\mu_h)^{1/2}]$ of the material in the holes, increases the plasma frequency in accord with Eq. (8).

We also calculate, using similar methods as outlined earlier, the dispersion relation for the coupling of light onto a circular hole textured surface, using a cylindrical (r,ϕ,z) coordinate system (Fig. 2). The cylindrical coordinate system is defined for one single circular hole, in a unit cell of the entire medium. In this case, the electric field in the holes has the following form:

$$E_r = \frac{E_1}{r}\cos(\varphi)J_1(k_c r)\exp[i(k_z z-\omega t)], \tag{12a}$$

$$E_\varphi = E_2\sin(\varphi)J_1'(k_c r)\exp[i(k_z z-\omega t)],$$
$$\text{where } 0<r<R \text{ and } R\ll\lambda. \tag{12b}$$

J_1 and J_1' represent the first-order Bessel function and its derivative. E_1 and E_2 are constants, where $E_2=-k_cE_1$, k_c is the cutoff wave number, and R is the hole radius. By matching the electrical field and the incident energy, we derive the electric fields in the effective medium as:

$$E' = \frac{\pi E_1[2-2J_0(k_cR)-k_cRJ_1(k_cR)]}{k_cD^2}, \tag{13a}$$

$$E'^2 = E_1^2\frac{\pi(P_{11}'^2-1)J_1^2(k_cR)}{4D^2}\frac{\mu_x}{\mu_h}, \tag{13b}$$

where P_{11}' is the first root of J_1', and $k_cR=P_{11}'$. We also derive the effective magnetic permeability coefficient and dielectric constant for the 2-D (x-y plane) circular hole textured isotropic film by equating the incident field and energy to the field and energy in the effective medium:

$$\mu_x=\mu_y=\frac{4\pi[2-2J_0(k_cR)-k_cRJ_1(k_cR)]^2}{D^2(P_{11}'^2-1)J_1^2(k_cR)k_c^2}\mu_h, \tag{14a}$$

$$\varepsilon_x=\varepsilon_y=\frac{D^2(P_{11}'^2-1)J_1^2(k_cR)k_c^2}{4\pi[2-2J_0(k_cR)-k_cRJ_1(k_cR)]^2}\varepsilon_h\left(1-\frac{\omega_{pc}^2}{\omega^2}\right). \tag{14b}$$

The surface plasma frequency (ω_{pc}), for a circle of radius R is then given by:

$$\omega_{pc}=\frac{P_{11}'c}{(\varepsilon_h\mu_h)^{1/2}}\frac{1}{R}, \tag{15}$$

and the dispersion relation is:

$$k_{cir}^2c^2=\omega^2+\frac{\mu_h}{\varepsilon_h}\left\{\frac{4\pi[2-2J_0(k_crR)-k_cRJ_1(k_cR)]^2}{D^2(P_{11}'^2-1)J_1^2(k_cR)k_c^2}\right\}^2 \times\omega^4\left(\frac{1}{\omega_{pc}^2-\omega^2}\right). \tag{16}$$

The bound nature, and differences, of the surface plasmon dispersion in the rectangular and the circular hole textured surfaces is evident in Fig. 3. The momentum mismatch in the circular case is smaller, which is closer to the free-space light vector (k_0). The physical origin of the lower mismatch arises from a more efficient electromagnetic wave coupling to a smaller number of dominant modes. It is hence posited that the surface texture can play a big role in the spoof SPP dispersion and will have to be reckoned with in plasmonic applications.

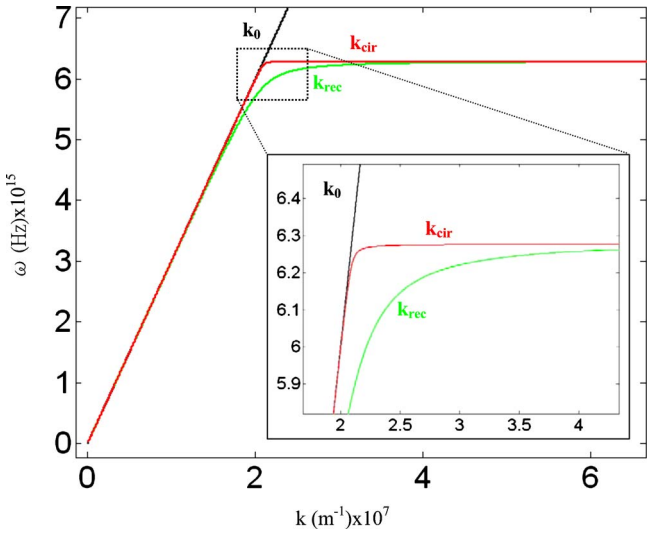

Fig. 3 A comparison of the $(\omega$-$k)$ dispersion for a rectangular (k_{rec}) and a circular (k_{cir}) patterned conducting film. The size of the circular holes (R=88 nm, D=350 nm) is chosen to match the plasmon frequency of the rectangular patterned surface (a=b=150 nm, D =350 nm). We observe that the SPPs for a rectangular patterned film have a larger momentum mismatch than the circular patterns.

We use a frequency-dependent term, the coupling parameter (CP), to calculate the momentum mismatch between rectangular (rec) and circular (cir) textured surfaces, untextured conducting film (k_f), and free-space photons k_0 as:

$$(CP)_{rec,cir}\equiv(k_{rec,cir}-k_0). \tag{17}$$

The momentum mismatch in electromagnetic wave-surface plasmon coupling is plotted as a function of frequency in Fig. 4, and it is concluded that the SPPs on a circular textured surface are less bound than in any other case considered. Since plasmonic circuitry consists of geometrical asperities/features, it would indeed be necessary to consider these aspects.

In summary, we have shown that the nature of surface texture in the subwavelength regime can play a significant role in determining the binding to the surface of the spoof plasmons. While the coupling efficiency of external light to the surface is suitably modified, one can also apply these principles for defect engineering, with the texture playing the role of the defect. For example, one can create surface plasmon bands of finite width by fine-tuning the geometry of the texture i.e., by alternating rectangular and circular holes. By combining the preceding texture-based dispersion relations with those of regular surface plasmons, we have a method of tuning surface plasmon frequencies. Experi-

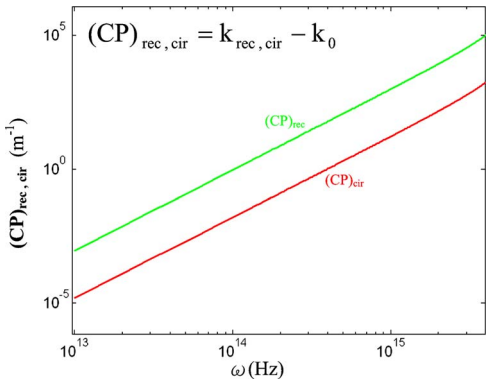

Fig. 4 The momentum difference between a bound SPP and the free-space light vector brought about by texturing a surface is quantified by the coupling parameter (CP). It is seen that at all frequencies, the SPPs on a circular textured surface have a smaller momentum difference compared to a rectangular textured surface. For these simulations, we use $a=b=150$ nm, and $r=88$ nm, and $D=350$ nm.

ments that explore these ideas will help in elevating the study of plasmon propagation on artificially engineered surfaces for nanophotonics and metamaterials applications.

Acknowledgments

The authors thank S. Mookherjea for many useful discussions. We gratefully acknowledge the financial support for this work by the National Science Foundation (NSF Grant Nos. ECS 0403589 and ECS 0643761).

References

1. S. Maier and H. A. Atwater, "Plasmonics: localization and guiding of electromagnetic energy in metal/dielectric strucrures," *J. Appl. Phys.* **98**, 011101 (2005).
2. T. W. Ebbesen, H. J. Lezec, H. F. Ghaemi, T. Thio, and P. A. Wolff, "Extraordinary optical transmission through sub-wavelength hole arrays," *Nature (London)* **391**, 667 (1998).
3. B. Liedberg, C. Nylander, and I. Lundstrom, "Surface plasmon resonance for gas detection and biosensing," *Sens. Actuators* **4**, 299–304 (1983).
4. A. Nemetz and W. Knoll, "Raman spectroscopy and microscopy with plasmon surface polaritons," *J. Raman Spectrosc.* **27**, 587 (1996).
5. K. Kneipp, Y. Wang, H. Kneipp, L. T. Perelman, I. Itzkan, R. R. Dasari, and M. S. Feld, "Single molecule detection using surface-enhanced Raman scattering (SERS)," *Phys. Rev. Lett.* **78**, 1667 (1997).
6. X. Luo and T. Ishihara, "Surface plasmon resonant interference nanolithography technique," *Appl. Phys. Lett.* **84**, 4780 (2004).
7. H. H. Lezec, A. Degiron, E. Devaux, R. A. Linke, L. Martin-Moreno, F. J. Garcia-Vidal, and T. W. Ebbesen, "Beaming light from a subwavelength aperture," *Science* **107**, 1895 (2002).
8. K. Okamoto, I. Niki, A. Shvartser, Y. Narukawa, T. Mukai, and A. Scherer, "Surface-plasmon-enhanced light emitters based on InGaN quantum wells," *Nat. Mater.* **3**, 601 (2004).
9. D. Crouse and P. Keshavareddy, "Polarization independent enhanced optical transmission in one-dimensional gratings and device applications," *Opt. Express* **15**, 1415–1427 (2006).
10. H. J. Lezec and T. Thio, "Diffracted evanescent wave model for enhanced and suppressed optical transmission through subwavelength hole arrays," *Opt. Express* **12**, 3629–3651 (2004).
11. E. Popov, S. Enoch, G. Tayeb, M. Neviere, B. Gralak, and N. Bonod, "Enhanced transmission due to nonplasmon resonances in one- and two-dimensional gratings," *Appl. Opt.* **43**, 999–1008 (2004).
12. F. J. Garcia De Abajo and J. J. Saenz, "Electromagnetic surface modes in structured perfect-conductor surfaces," *Phys. Rev. Lett.* **95**, 233901 (2005).
13. B. Hou, H. Hang, W. Wen, C. T. Chan, and P. Sheng, "Microwave transmission through metallic hole arrays: surface electric field measurements," *Appl. Phys. Lett.* **89**, 131917 (2006).
14. Q. Cao and P. Lalanne, "Negative role of surface plasmons in the transmission of metallic gratings with very narrow slits," *Phys. Rev. Lett.* **88**, 057403 (2002).
15. S. Maier and H. A. Atwater, "Plasmonics: localization and guiding of electromagnetic energy in metal/dielectric structures," *J. Appl. Phys.* **98**, 011101 (2005).
16. W. L. Barnes, A. Dereux, and T. W. Ebbesen, "Surface plasmon subwavelength optics," *Nature (London)* **424**, 824 (2003).
17. H. Raether, *Surface Plasmons*, Springer-Verlag, New York (1988).
18. J. R. Sambles, G. W. Bradbery, and F. Yang, "Optical excitation of surface plasmons: an introduction," *Contemp. Phys.* **32**, 173 (1991).
19. J. B. Pendry, L. Martin-Moreno, and F. J. Garcia-Vidal, "Mimicking surface plasmons with structured surface," *Science* **305**, 847 (2004).
20. A. P. Hibbins, B. R. Evans, and J. R. Sambles, "Experimental verification of designer surface plasmon," *Science* **308**, 670 (2005).
21. C. Kittel, *Introduction to Solid State Physics*, John Wiley, New York (1996).
22. D. M. Pozar, *Microwave Engineering*, 2nd ed., John Wiley & Sons, New York (1998).

Biographies and photographs not available.